2011-11

Modeling epileptogenesis and temporal lobe epilepsy in a non-human primate

Epilepsy Research, Amsterdam : Elsevier BV, v. 96, n. 1/2, p. 45-57, Nov. 2011
http://www.producao.usp.br/handle/BDPI/49812

Epilepsy Research (2011) **96**, 45—57

journal homepage: www.elsevier.com/locate/epilepsyres

Modeling epileptogenesis and temporal lobe epilepsy in a non-human primate

P. Perez-Mendes[a,b,1], M.M. Blanco[a,b,1], M.E. Calcagnotto[a,b], S.M. Cinini[a,b], J. Bachiega[a,b], D. Papoti[a,b], L. Covolan[a,b], A. Tannus[a,b], L.E. Mello[a,b,*]

[a] *Departamento de Fisiologia, Universidade Federal de São Paulo, Brazil*
[b] *Instituto de Física de São Carlos (IFSC), Universidade de São Paulo, Brazil*

Received 26 January 2011; received in revised form 29 March 2011; accepted 29 April 2011
Available online 26 May 2011

KEYWORDS
Pilocarpine;
Temporal lobe epilepsy;
Marmosets;
Status epilepticus

Summary Here we describe a new non-human primate model of temporal lobe epilepsy (TLE) to better investigate the cause/effect relationships of human TLE. Status epilepticus (SE) was induced in adult marmosets by pilocarpine injection (250 mg/kg; i.p.). The animals were divided in 2 groups: acute (8 h post-SE) and chronic (3 and 5 months post-SE). To manage the severity of SE, animals received diazepam 5 min after the SE onset (acute group: 2.5 or 1.25 mg/kg; i.p.; chronic group/; 1.25 mg/kg; i.p). All animals were monitored by video and electrocorticography to assess SE and subsequent spontaneous recurrent seizures (SRS). To evaluate brain injury produced by SE or SRS we used argyrophil III, Nissl and neo-Timm staining techniques. Magnetic resonance image was also performed in the chronic group. We observed that pilocarpine was able to induce SE followed by SRS after a variable period of time. Prolonged SE episodes were associated with brain damage, mostly confined to the hippocampus and limbic structures. Similar to human TLE, anatomical disruption of dentate gyrus was observed after SRS. Our data suggest that pilocarpine marmoset model of epilepsy has great resemblance to human TLE, and could provide new tools to further evaluate the subtle changes associated with human epilepsy.

Introduction

Mesial temporal lobe epilepsy (TLE) is the most common form of human epilepsy (Engel and Pedley, 1997). Frequently used animal models of TLE are the kindling model (Goddard, 1967; McNamara, 1986; Pinel and Rovner, 1978) where repetitive daily stimulation eventually leads to the emergence of spontaneous recurrent seizures (SRS); and the kainate (Ben-Ari et al., 1980; Cavalheiro et al., 1982; Hellier et al., 1998) or the pilocarpine models (Leite et al., 1990; Turski et al., 1983) where administration of a chemical agent leads to an

* Corresponding author at: Department of Physiology, Universidade Federal de São Paulo, Rua Botucatu, 862, 5° andar, Ed. Ciências Biomédicas, CEP 04023-062, São Paulo, Brazil.
Tel.: +55 11 5579 2033; fax: +55 11 5579 2033.
E-mail address: lemello@unifesp.br (L.E. Mello).
[1] These authors contributed equally to this work.

0920-1211/$ — see front matter © 2011 Elsevier B.V. All rights reserved.
doi:10.1016/j.eplepsyres.2011.04.015

intense and lasting epileptic seizure (status epilepticus, SE) followed by SRS after a few weeks. Seizures in rodents also can be induced by domoic acid, another chemical agent acting on glutamate/kainate receptors (Doucette et al., 2004; Tasker et al., 1996). However, the domoic acid is extremely toxic to humans (Perl et al., 1990) and non-human primates (Perez-Mendes et al., 2005; Scallet et al., 1993; Tryphonas and Iverson, 1990; Tryphonas et al., 1990).

A number of differences between rodents and primates in terms of hippocampal anatomy and physiology (e.g., neurogenesis, basal dendrites on granule cells) are often cited to explain the discrepancies between rodent models of epilepsy (p.e., pilocarpine, kainate, kindling) and human epilepsies. Few studies were performed attempting to develop non-human models of TLE (Gunderson et al., 1999; Soper et al., 1978; Wada and Osawa, 1976; Wada et al., 1974). However the treated animals did not develop chronic spontaneous recurrent seizures and often the brain damage was diffuse resulting in multiple foci outside the limbic system. The use of pilocarpine in non-human primates as a model of epilepsy could provide new insights concerning the human TLE. To properly evaluate the causes and consequences associated with human TLE we sought to develop a non-human primate model of temporal lobe epilepsy.

Materials and methods

Animals

Adult marmosets (*Callithrix jacchus*), males and females (2—8 years-old; 250—400 g; $n = 28$) were kept under conditions of controlled temperature, illumination (12/12-h cycles) and appropriate diet. All experimental protocols were performed at the Laboratory of Primates of UNIFESP (Universidade Federal de São Paulo) and were approved by the Animal Care and Use Committee of UNIFESP in accordance with the National Institutes of Health guidelines on animal care.

Electrodes implantation for electrocorticography (ECoG)

The marmosets were sedated with diazepam (1.0 mg/kg; i.m.; Cristália, São Paulo, Brazil) and then anesthetized 10 min later with ketamine 10% (1 mg/kg; i.m.; Agener União, São Paulo, Brazil) and xylazine 2% (0.5 mg/kg; i.m.; Bayer, São Paulo, Brazil). Additional half-dose of anesthesia was given when necessary. Subdural telemetry bipolar electrodes (Data Sciences International, St. Paul, MN, USA) were implanted in the motor cortex of marmosets. For acute experiments, the telemetry bipolar electrode (DSI transmitters-TA11CTAF40) (Data Sciences International, St. Paul, MN, USA) was placed subcutaneously in the intra scapular region of each animal through an infra scapular incision of 3 cm. The electrode was subcutaneously introduced from the intra-scapular region and guided to the surgical incision made at the skull region. To avoid postoperative infection and pain, all animals received broad spectrum veterinarian antibiotic (0.1 mL/kg; i.m.; Fort Dodge, São Paulo, Brazil) and analgesic banamine® (1 mg/kg; i.m.; Schering-Plough, São Paulo, Brazil).

Pilocarpine injection

The animals were kept isolated in metal cages for 2 days before the drug injection. Sixteen days after electrode implantation, marmosets were injected with scopolamine methyl bromide (1 mg/kg; i.p.; Sigma, St. Louis, USA) and 20 min later, with pilocarpine hydrochloride (250 mg/kg; i.p.; Merck, São Paulo, Brazil). The control group ($n = 2$) received saline 0.9% instead of pilocarpine. To avoid possible deaths, the animals received sub-therapeutic dose of diazepam 5 min after SE (Perez-Mendes et al., 2005). For the acute study, 20 animals with SE received diazepam at 2.5 mg/kg; i.p. ($n = 12$) or 1.25 mg/kg; i.p. ($n = 8$). For the chronic study, 10 animals with SE received diazepam at 1.25 mg/kg; i.p. The animals remaining in SE after 4 h received a supplementary dose of diazepam (1.25 mg/kg; i.p.). Immediately after the SE the animals received glucose solution (1 glucose 50%: 4 saline 0.9%; 1 mL s.c.) and were kept warmed. The normal diet was restarted when the animals become alert.

Video/ECoG

One day before the pilocarpine injection the animals were monitored with ECoG for 24 h (baseline). The animals from the acute group were monitored for 8 h post-pilocarpine injection (Video/ECoG for 6 h consecutively, and with ECoG only, for the final 2 h). The animals from the chronic group were monitored with Video/ECoG for 24 h/day for 7 consecutive days post-pilocarpine injection followed by 7 consecutive days 24 h/day during alternated weeks during 19 consecutive weeks. For the chronic group, the animals with SE that survived over 48 h were then divided in 2 chronic groups: one observed for 3 months (G3m, $n = 3$) and the other for 5 months (G5 m, $n = 4$). During the chronic follow up we evaluated the rate and the electrographic pattern of SRS. The pro-convulsive behavior after pilocarpine administration was evaluated according to the modified Racine scale from I to V described previously (Bachiega et al., 2008; Racine et al., 1972) as follows:

I. Facial automatisms, including salivation, ''mouth cleaning-like'' behavior, and tongue automatisms.
II. Facial movements, head clonus, and head shakes.
III. Forelimb clonus.
IV. Bilateral forelimb clonus, rearing, arched body posture, straub tail.
V. Generalized clonic seizures and postural impairment.

We evaluated the stages according its latency and duration. ECoG was acquired with Data Sciences Telemetry System (St. Paul, MN, USA) and the electrographic pattern of SE and SRS were analyzed by ART 3.0 software.

Argyrophil III staining

All animals from the acute group were deeply anesthetized (thionembutal, 50 mg/kg; i.p.; Cristália, São Paulo, Brazil) 8 h after SE and perfused as described previously (Covolan and Mello, 2000) The brains were kept 48 h inside the skull. Later, they were removed and post fixed for a week in the same fixative and then placed in sucrose 30% for 48 h. After cryoprotection, 60-μm thick coronal sections were cut using the cryostat and the Argyrophil III staining (to identify neuronal injury expressed as presence of dark neurons) was performed as described elsewhere (Covolan and Mello, 2000). The dark neurons were evaluated in the brain regions (plates) based on the marmoset brain atlas (Stephan et al., 1980) (2 slices/plate/animal). The rostral (plates A11.5, A10.5 and A9.5) medial (plates A8.0, A6.0 and A5.0) and caudal (plates A4.0 and A2.0) regions of the brain were analyzed. To determine the neuronal damage we used a microscope (Olympus BX50; $\times$100) connected to a computer (Macintosh-PowerMac 8600/200). The argyrophilic staining was scored as presence of dark neurons based on the percentage of brain structure with dark cells (Covolan and Mello, 2000) as following: 0: 0%, 0.5: 10%, 1.0: >10—25%, 1.5: >25—45%, 2.0: >45—55%, 2.5: >55—75%, and 3.0: >75%. Two persons blinded to the treatment conditions performed the evaluation.

Nissl staining (Cresyl violet)

Coronal brain slices of 60-μm from the acute and chronic groups were stained with cresyl violet to visualize the neuronal loss and cell dispersion (within hippocampal pyramidal and dentate granule cell (DGC) layers). The analysis was made based on the marmoset brain atlas (Stephan et al. 1980). We performed a qualitative analysis of rostral (plates A7.0—A6.0), medial (plates A5.0—A4.0), and caudal (plates A3.0—A2.0) regions of hippocampal hilus, in 3 sections/plate/animal. To measure the cell dispersion of CA3 pyramidal and DGC layers we used the same plates described above, in 5 sections/plate/animal (3—5 measurements each layer) using the software NIH Image 1 .62. The analysis the width of the DGC layer was assessed in the narrowest and widest zones of DG (e.g., in the curved zones and especially in the folded hippocampus). For each zone, the width was the result of an average of 8 values. For each case, the width of the DGC layer was assessed 16 times bilaterally in the hippocampus.

Magnetic resonance image (MRI)

MRI was performed in animals during the chronic period at the Physics Institute of USP (Universidade de São Paulo) in São Carlos. The images were acquired from animals, already perfused, in a 2.0 T MRI for animals. The acquisition protocol was previously tested in a normal control animal to standardize the method. MRI was performed in chronic animals (G3m, $n = 1$ and G5m, $n = 3$), NSE ($n = 1$) and control ($n = 1$). The acquisition protocol was the following: FOVr (field of view for reading) = 4 cm, FOVp (field of view for phase) = 4 cm, TR (time of repetition) = 2000 ms, TE (time of echo) = 75 ms, Nr (number of points for reading) = 256, Np (number of points for phase) = 256, number of mean = 20, Number of slices = 19, thickness of slices = 1.5 mm, distance between slices = 2 mm, total acquisition time = 2 h and 50 min.

Neo-Timm staining

While under deep anesthesia the chronic animals were transcardially perfused with (i) 200—300 mL phosphate buffer, (ii) 300 mL 0.1% Na_2S in Millonig's buffer, and (iii) 300—400 mL 4% paraformaldehyde in PBS 0.01 M, pH 7.2, 4 °C. The brains were removed and placed in sucrose 30% for 48 h. Next, 30-μm thick coronal sections were cut with a cryostat and developed according to standard neo-Timm protocol as described previously (Mello et al., 1993). The intensity of neo-Timm staining in the supragranular layer of dentate gyrus (DG) was subjectively scored (Tauck and Nadler, 1985) from 0 (no staining) to 3 (densely and continuous staining through the DGC layer). All rostro-caudal axis of hippocampal complex were evaluated. The analysis of the hippocampus was performed by 2 persons blinded to the treatment conditions.

Immunohistochemistry

Immunohistochemistry for glial fibrillary acidic protein (GFAP)-positive cells (astrocyte marker) was performed using the ABC method. Coronal brain sections from chronic epileptic, NSE and control groups were incubated overnight with primary polyclonal antibody against GFAP (1:2000; DakoCytomation) followed by incubation with the appropriate secondary biotinylated antibody (1:600; Vector Laboratories; anti-rabbit). Briefly, coronal sections (30 μm) were rinsed in potassium PBS, treated with 3% H_2O_2, and incubated overnight with 0.1% Triton X-100 plus PBS solution and primary antibody. Sections were rinsed and incubated in avidin—biotin complex (Elite ABC kit, Vector Laboratories), and developed with diaminobenzidine. Sections were analyzed by conventional microscopy. GFAP-stained sections were quantitatively assessed as follows: score 0: no obvious expression, score 1: obvious expression involving 10—25% of the region, score 2: obvious expression involving 40—60% of the region, and score 3: >80% the expression in the regions of interest. Assessment was performed in hilar regions, CA1, CA3, subiculum, temporal cortex, frontal cortex, entorhinal cortex, hypothalamus and thalamus in four sections per animal.

Statistics

The data was analyzed using Student's *t*-test and ANOVA followed by Tukey—Kramer post hoc test with significance level of $P < 0.05$. Results were presented as the mean ± SEM.

Results

Pilocarpine triggers SE

To evaluate whether pilocarpine is capable of inducing SE in marmosets, the animals were monitored by a Video/ECoG telemetry system. We observed that pilocarpine was able to evoke a number of different convulsive behavior prior the SE. All 30 animals injected with pilocarpine had at least 2 episodes of convulsive behavior stages I—IV (Bachiega et al., 2008; Racine et al., 1972) progressively. The beginning of SE was characterized by convulsive behavior stage IV. Twenty-four out of the 30 animals (80%) injected with pilocarpine developed SE. Four of them died during SE and 2 died 48 h and 2 months after SE and six animals did not develop SE (NSE). There was no association between latency/duration of these convulsive stages and the subsequent development of SE or duration of SE. Two out of 6 NSE animals presented only a single tonic—clonic seizure and recovered in a few minutes and have no SRS during the ECoG recordings. Control animals did not have any convulsive behavior. To more completely characterize the SE in marmosets we focused our analysis on the latency, duration and ECoG patterns. All animals received diazepam 5 min after SE started (i.e., after convulsive behavior stage IV). The latency for the beginning of SE was 16.8 ± 4.0 min ($n = 24$). The duration varied from 1 h to 3 h (2.2 ± 0.4 h) for animals treated with 2.5 mg/kg diazepam ($n = 7$) and from 2 h to 9 h (5.9 ± 1.0 h) for animals treated with 1.25 mg/kg ($n = 11$) (Student's *t*-test, $P < 0.01$) (Fig. 1A). According to the ECoG pattern we classified the SE in 5 phases as following: I: high amplitude, high frequency spikes (≥1.0 mV; 13—18 Hz); II: high amplitude, low frequency spikes (≥1.0 mV; 3—8 Hz) with short period of high frequency (13—18 Hz); III: bursts of 10 Hz followed by a period of high frequency activity; IV: small burst of low amplitude followed by high frequency activity; V: predominantly attenuated as compared to phase IV but with short period of high amplitude activity; post-ictal period: attenuation of baseline (Fig. 1B). The ECoG recording became normal around 2 h after the end of phase V. This ECoG pattern was observed in all animals, going from phase I to V (Fig. 1C). The animals treated with 2.5 mg/kg of diazepam had shorter duration of phase IV (2.1 ± 0.45 h) when compared with those treated with diazepam 1.25 mg/kg (0.7 ± 0.3 h) (Student's *t*-test, $P < 0.05$). Thus, diazepam could be responsible for the attenuation of amplitude and duration of the epileptiform activity. The duration of the post-ictal period was variable.

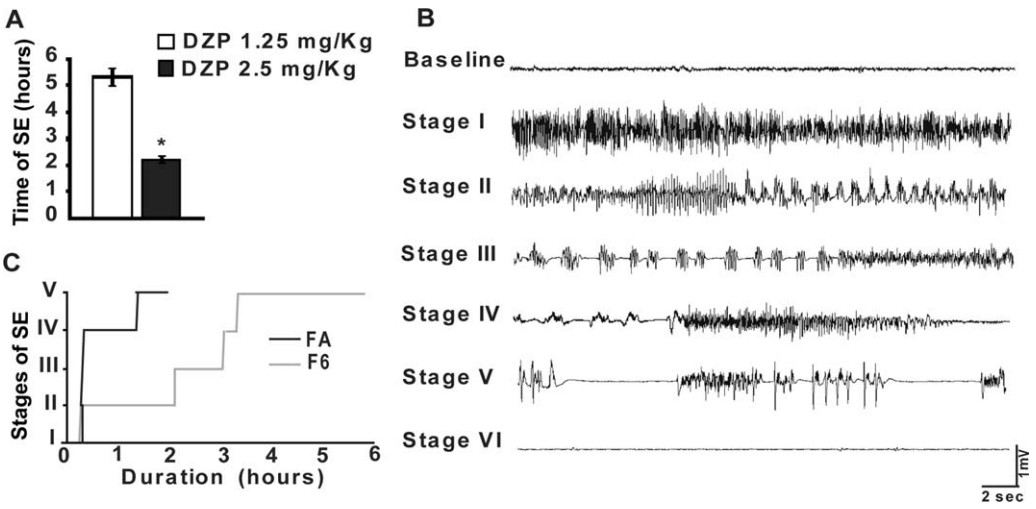

Figure 1 Characterization of Pilocarpine-induced SE in marmosets. (A) Plots of SE duration for different diazepam doses. (B) ECoG recordings showing the phases of SE in marmosets. (C) Characterization of the duration of the different SE phases in 2 representative animals (FA and F6: marmosets from acute and chronic group, respectively) as following: I: high amplitude, high frequency spikes, II: high amplitude, low frequency spikes with short period of high frequency spykes, III: bursts of 10 Hz followed by a period of high frequency activity, IV: small burst of low amplitude followed by high frequency activity, and V: predominantly attenuated with short period of high amplitude activity; followed by post-ictal period (VI) of attenuated baseline. *Student's *t*-test; $P < 0.05$.

To evaluate the early and late consequences of SE we divided the animals in 2 groups following the SE, acute and chronic groups.

Prolonged SE is required to promote injury

Given the ability of pilocarpine to induce SE in marmosets we then investigated the association between SE and acute brain damage. To address this issue we evaluated neuronal damage in several marmosets' brain areas using the argyrophil III silver (Gallyas et al., 1992; Ishida et al., 1999) and the Nissl stainings. Sixteen marmosets from the acute group were analyzed ($n = 11$ SE, 3 NSE and 2 controls). Argyrophilic dark neurons were detected in several brain structures of animals after SE, mainly in the limbic structures (Supplementary Table 1). Negligible cell injury was found in the NSE (Fig. 2A—D) and control groups (data not shown). From the SE group, the 6 animals receiving higher doses of diazepam (2.5 mg/kg), had shorter duration of SE (1—3 h) and less widespread brain damage (32 different brain structures with injured cells) (Fig. 2E—H and Supplementary Table 1) than the 5 animals that received lower doses of diazepam (1.25 mg/kg; 2—8 h; 52 different brain structures with injured cells) (Fig. 2I—L and Supplementary Table 1). Overall, there was no further increase in neuronal damage in animals with longer SE duration (4—8 h). Given the thickness of the brain slices (60-μm; required for the silver staining) available for the Nissl staining we performed a qualitative analysis of the cell loss (Bethmann et al., 2008; Covolan and Mello, 2000). We did not observe cell loss in the CA2 hippocampal subregion in any group of animals. However, neuronal loss in hippocampal was observed in the regions of CA1, CA3 and hilus of animals post-SE ($n = 11$; acute group) but not in the control ($n = 2$) or NSE ($n = 3$) groups. These data clearly indicate that pilocarpine-induced SE promotes acute brain damage in marmosets. The lower dose of diazepam, as expected, resulted in more severe and extended neuronal injury.

Spontaneous seizures develop after SE

Since SE duration of 60 min causes great neuronal damage in rodents (Covolan and Mello, 2000), we decided to lower the dose of diazepam (1.25 mg/kg) in order to evaluate the occurrence of SRS in the chronic group.

To assess whether pilocarpine-induced SE in marmosets was followed by SRS we performed continuous Video/ECoG recordings over a period of several weeks. Eight out of 10 marmosets injected with pilocarpine developed SE with a variable duration of 4—9 h. SRS were observed in 5 out of 7 animals over the 19 weeks of observation. To characterize the SRS we evaluated the ECoG pattern and the behavioral manifestation. We observed 4 different types of spontaneous electrographic seizures, according the latency, frequency and amplitude of epileptiform discharges (Fig. 3A). The most frequent seizure type observed in the ECoG was type 4 (Fig. 3B). The latency for SRS after SE varied from a few days ($n = 2$) to several weeks (5 weeks, $n = 1$; 7 weeks, $n = 1$ and 15 weeks, $n = 1$). SRS frequency was higher in the initial weeks with a gradual reduction in the following weeks (Fig. 3C). There was no EMG alteration during the seizures type 1, 2, or 3 and the body temperature measured did not change in any of the seizure types. Seizure type 1 had duration of 6.83 ± 0.13 s, type 2, 13.08 ± 1.21 s, type 3, 24.50 ± 1.71 s, and type 4, 79.90 ± 0.66 s. We did not observe any clinical or electrocorticographic manifestation of seizures in the animals without SE. The behavioral manifestation was evident only during seizure type 4 and was characterized by grooming followed by progressive clonic movements of all four limbs and loss of posture. The

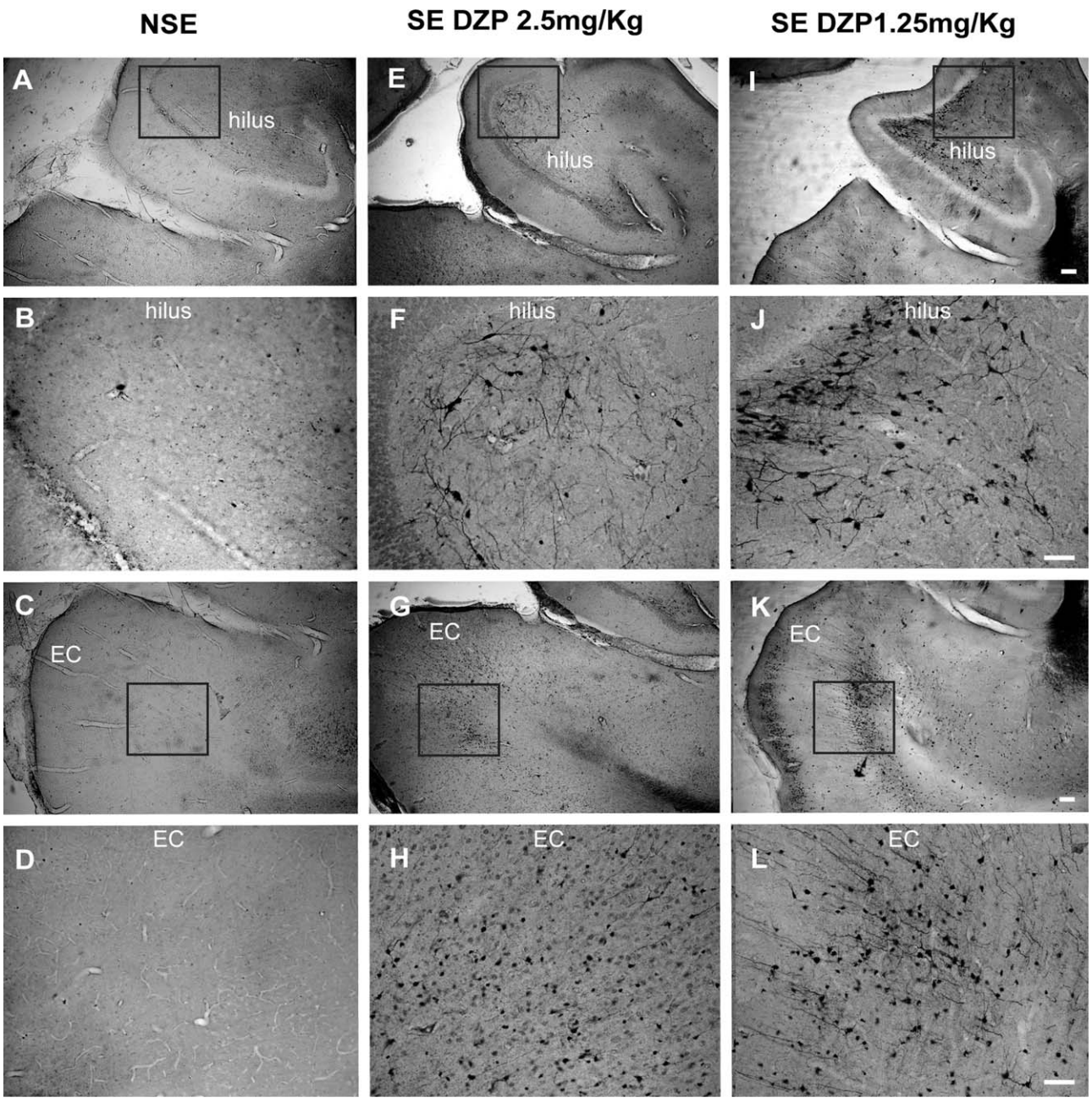

Figure 2 Cell death in hippocampal formation of SE animals. Argyrophil III staining of hippocampal hilus (A, E, I and higher magnification insets B, F, J) and entorhinal cortex (C, G, K and higher magnification insets D, H, L) of a NSE, (A—D) SE animal receiving diazepam 2.5 mg/kg (E—H) and SE animal receiving diazepam 1.25 mg/kg (I—L). The presence of dark cells in the SE animal injected with 1.25 mg/kg diazepam is more intense than those injected with 2.5 mg/kg diazepam. No cell damage in NSE animal. Scale bar: A, E, I, C, G, K: 100 μm; B, F, J, D, H, L (insets): 50 μm. EC: entorhinal cortex.

post-ictal period lasted for about 3—4 h and was characterized by mydriasis, relative immobility and lack of responsiveness to sound stimulation. Taking altogether, we conclude that pilocarpine-induced SE in marmosets is followed by SRS, after a variable latent period, frequency and seizure pattern. We are did not observe significant interictal discharges that could be measured on the ECoG during the time recorded.

Brain damage is confined to the hippocampus and limbic structures in the chronic phase

We demonstrated above that SE was capable to induce acute brain damage in marmosets. To fully evaluate whether chronic seizures are associated with anatomical, morphological and cellular changes in the brain, we performed MRI of the intact brains; and Nissl and neo-Timm stainings of the

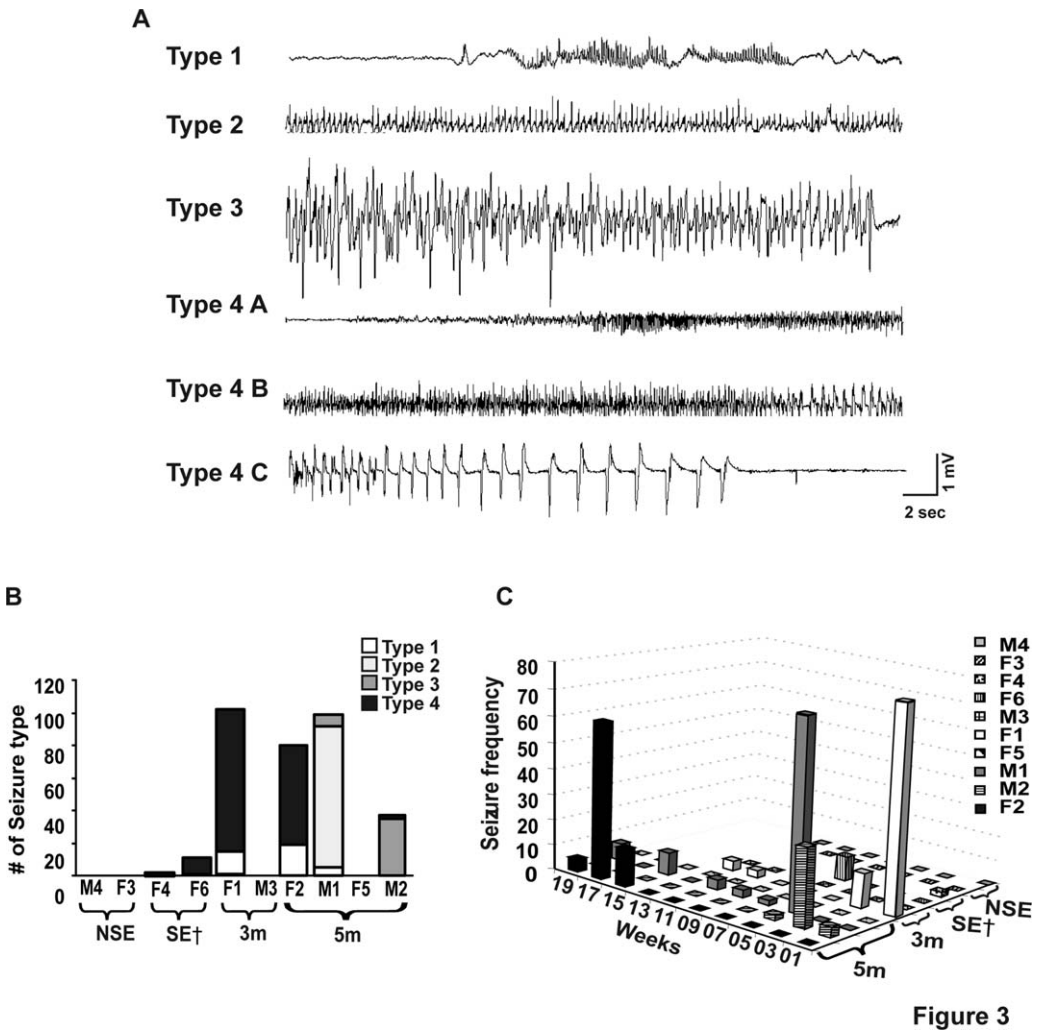

Figure 3

Figure 3 Characterization of SRS during the chronic phase post pilocarpine-induced SE. (A) Electrographic representation of the 4 different seizure types (a, b and c represent the same single seizure episode); (B) Characterization of the different seizure types for each chronic animal; (C) Frequency of SRS for all chronic animals distributed over time.M4 to F2: animal codes; 3 m and 5 m:Chronic group with 3 and 5 months follow up respectively; SE†: Animals with SE who had died; NSE: group of animals without SE.

brain sections from marmosets after the chronic period of 3 and 5 months.

MRI was performed in 6 animals (4 SRS, 1 NSE and 1 control). The morphological alterations of the hippocampus from these animals are described in Supplementary Table 2 The M3 animal that was assessed by MRI at 3 months after the SE (G3m chronic epileptic animal) histologically exhibited little neuronal loss in CA1, CA3 and hilus and discrete mossy fiber sprouting. At the MRI level, no alterations were observed in Control (Fig. 4A and B), NSE (Fig. 4C and D) and G3m (Fig. 4E and F). Morphological alterations were observed in hippocampal structures only in 2 animals from G5m and were characterized by increased T2 signal of the hippocampal region with bilateral mesial atrophy (Fig. 4G and H). At histology, one of these G5m animals (M2) presented neuronal loss in CA1 CA3 and hilus with, severe cell dispersion in CA3 and GDG and severe mossy fiber sprouting. In addition this animal exhibited DG malformation. The other of these, animal F5, exhibited little neuronal loss in the hilus and cell dispersion in CA3; however did not present mossy fiber sprouting. No alterations were found in other brain structures.

As we observed alterations at the MRI similar to the hippocampal sclerosis seen in TLE, we performed immunohistochemistry for GFAP to evaluate the presence of gliosis in the hippocampus of the epileptic marmosets. We performed a qualitative analysis of GFAP positive cells in several brain structures such as, hilus, CA1, CA3, subiculum, entorhinal cortex, temporal cortex, frontal cortex, thalamus and hypothalamus of epileptic animals (G3m and G5m), NSE and controls. However, the GFAP expression was similar for all groups (Supplementary Fig. 1 and Table 3).

Nissl staining revealed cellular dispersion, neuronal loss and morphological changes in hippocampal areas of chronic animals. The cellular dispersion was significantly higher in the DGC layer of animals from G5m ($182 \pm 17\,\mu m$), when compared with all other groups, G3m ($130 \pm 7.0\,\mu m$) and controls ($135 \pm 10\,\mu m$; ANOVA—Tukey—Kramer test, $P < 0.05$; Fig. 5A). There was also a significant increase in thickness of DGC layer in animals with SRS from both groups (G3m

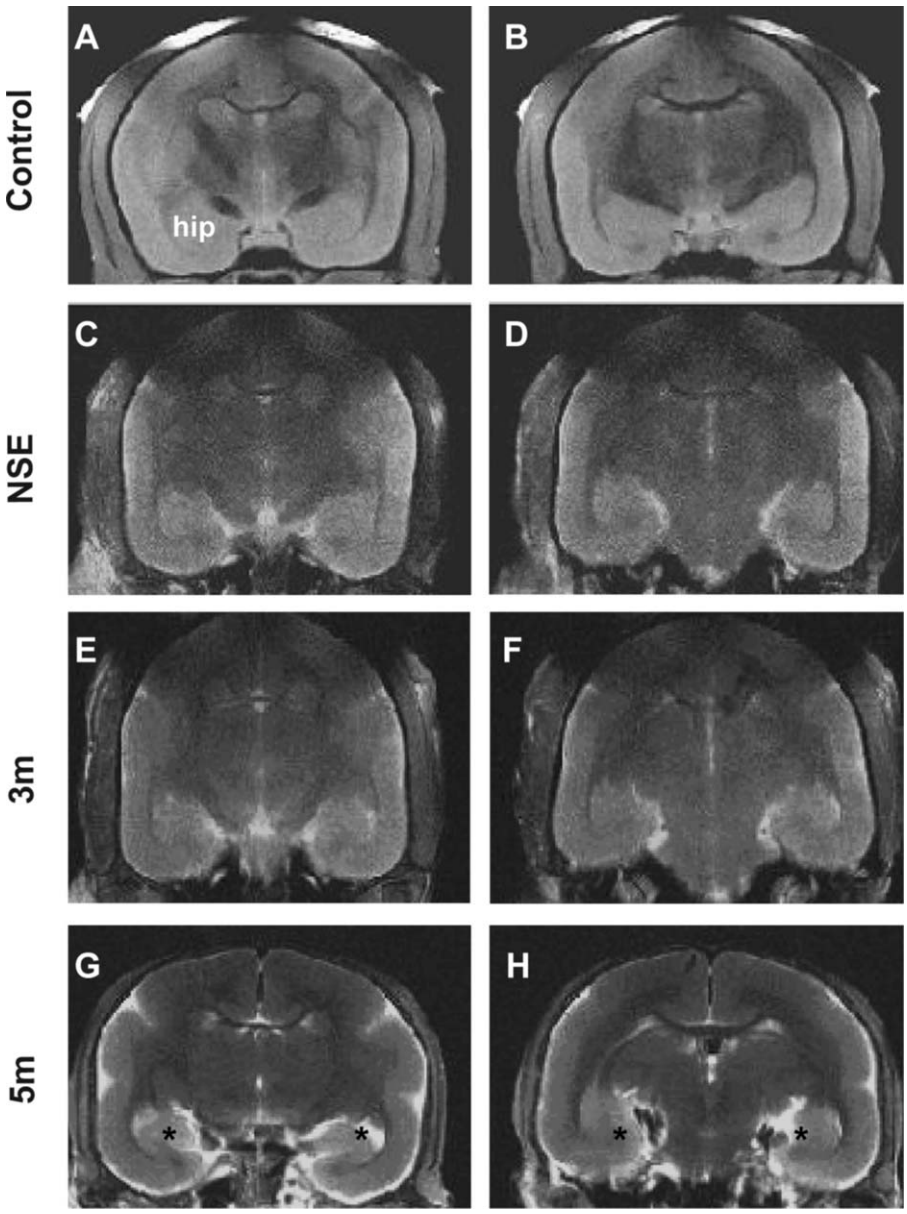

Figure 4 MRI features of marmosets brain during the chronic period after pilocarpine-induced SE. Coronal MRI sections in T2 sequence of control (A and B), NSE (C and D) as well as 3 months (E and F) and 5 months (G and H) after SE. Note the bilateral hippocampal region with hyper signal associated with mesial atrophy in G and H (*); hip: hippocampus.

and G5m) ($172 \pm 17\ \mu m$) when compared with animals without SRS ($133 \pm 7.6\ \mu m$; Student's t test, $P < 0.05$; Fig. 5B). Neuronal loss in CA1, CA3 hippocampal regions and hilus was detected in the epileptic but not in NSE or control groups ($n = 5$). In the hilar region both epileptic groups had significantly less neurons (G3m, 10 ± 3.5 neurons/$100\ \mu m^2$; and G5m, 10 ± 2.5 neurons/$100\ \mu m^2$) than the control group (21.5 ± 1.5 neurons/$100\ \mu m^2$; ANOVA—Tukey—Kramer test, $P < 0.05$; Fig. 5C). In addition, there was a significant neuronal loss in the hilar region in animals with SRS (8.2 ± 1.9 neurons/$100\ \mu m^2$) when compared with animals without SRS (20 ± 1.5 neurons/$100\ \mu m^2$; Student's t test, $P < 0.01$; Fig. 5D).

By the morphological analyses of the hippocampus, we observed an interesting malformation in the DGC layer similar to that was described previously in humans with TLE (Sloviter et al., 2004). We observed the DG malformation in 2 out of 6 chronic epileptic animals. This malformation, observed only in the G5m group, was characterized by invaginations and lateral displacement of the DGC layer, mainly in the posterior plates with no additional morphological alteration in the hippocampus (Fig. 6E and F). These grossly distorted DGC layer were never seen in controls (Fig. 6A and B), NSE animals (Fig. 6C and D) or in the G3m group. We did not observe cell displacement in other areas of the hippocampal formation. Neo-Timm staining showed MFS in the DG in some but not all of the animals from both chronic groups (Fig. 7C and D). The presence or absence of SRS did not seem to be affected by the presence or not of MFS (animal M3 showed MFS but no SRS, whereas in

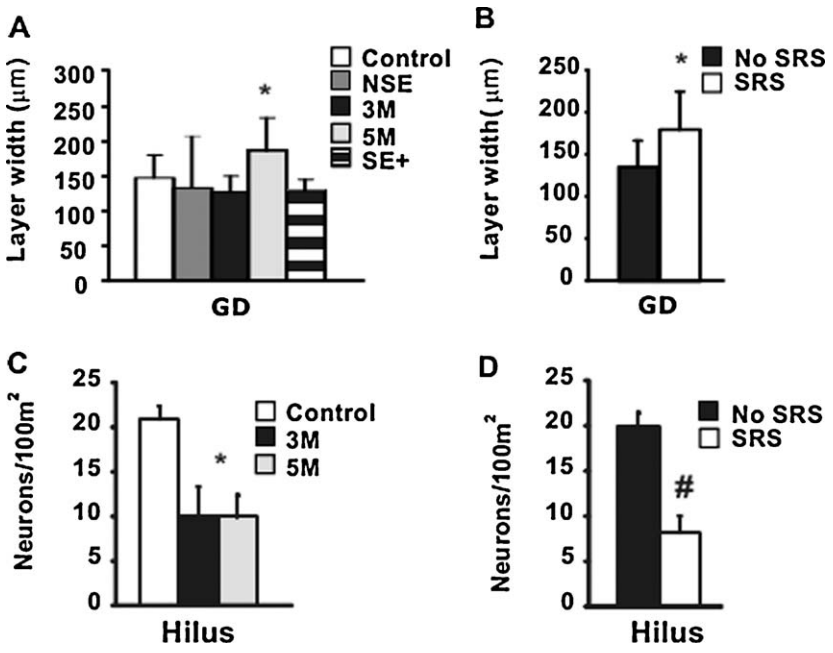

Figure 5 Cellular dispersion and neuronal loss in hippocampus of marmosets evaluated by Nissl staining. Quantification of cell dispersion in DGC layer comparing all chronic groups (A) and only animals of the SE group divided according to presence or absence of SRS (B). Plots showing neuronal loss in the hilus of both epileptic groups (G3m and G5m) when compared with controls (C) and in the animals with SRS when compared with animals without SRS (D). $^{*}P < 0.05$ and $^{\#}P < 0.01$.

contrast animal M1 exhibited SRS but no MFS). MFS was not found in control (Fig. 7A and B) or NSE groups (data not shown). Supplementary Table 2 shows the overall morphological alterations observed in the hippocampal formation for all groups. In summary, when compared with other rodent models of epilepsy, the marmosets with chronic SRS exhibited brain damage restricted mainly to the hippocampus and limbic structures.

Discussion

Experimental animal models of mesial TLE have helped to elucidate the morphological and functional alterations of hippocampal sclerosis associated with epilepsy. Here we describe a new model of TLE induced by pilocarpine in a non-human primate (*C. jacchus*). Our main findings in this model include the following: (i) pilocarpine was able to induce SE in marmosets, (ii) prolonged SE was needed to cause brain injury, (iii) the SE was followed, by SRS associated with brain damage mostly confined to the hippocampus and limbic structures, and (iv) gross morphological distortions were found in the DG in chronic animals and may have occurred as a consequence of the epileptic condition.

The present work follows our previous attempt to create a non-human primate model of epilepsy by using domoic acid (Perez-Mendes et al., 2005). Due to the high SE-associated mortality in marmosets prompted us to treat the animals with diazepam at a earlier time point (5 min after SE onset) than used for rats (~60 min after SE onset) (Mello et al., 1993). Despite the earlier time point of SE titration, diazepam did not fully abolish the SE and the animals still present cell damage and most subsequently developed SRS. In the pilocarpine and kainate models of epilepsy in rodents, a severe episode of SE is essential for the subsequent development of SRS (Goffin et al., 2007; Lemos and Cavalheiro, 1996). By managing the severity of the SE, injecting sub-therapeutic doses of diazepam after the SE onset, one can decrease mortality without decreasing the development of epilepsy (Cunha et al., 2009; Gao et al., 2007; Hellier et al., 1998; Mello et al., 1993; Treiman et al., 1998; Walton and Treiman, 1988). The immediate seizures following pilocarpine injection in marmosets were similar to those described in pilocarpine-treated rodents (Racine et al., 1972; Turski et al., 1983). Development of SE after pilocarpine was markedly faster in marmosets than in rodents, that developed motor limbic seizures over 1—2 h and built up progressively into limbic SE (Turski et al., 1983).

As expected, the administration of lower dose of diazepam resulted in more extensive brain damage than higher dose. We observed a more diffuse degeneration pattern across the entorhinal cortex layers in animals receiving highest dose of diazepam (Fig. 2G and H; 2.5 mg), and an intense degeneration pattern only in superficial and deeper entorhinal cortex layers associated with the lowest dose of diazepam (Fig. 2K and L; 1.25 mg). Several studies have shown the different connections between the superficial layers II—III and deep V—VI of entorhinal cortex with different regions of neocortex, GD, hippocampal formation and subiculum (Dolorfo and Amaral, 1998; Kloosterman et al., 2003; Kobayashi et al., 2003; Kohler, 1986; van Haeften et al., 2003). The more intense neuronal death in those regions, the more specific will be the cell death in correspondent entorhinal cortex layers. That could explain our findings of less cell death in general brain structures associated with a diffuse and less intense damage in entorhinal cortex in epileptic animals receiving the highest diazepam dose; and more cell death in hippocampal and cortical areas

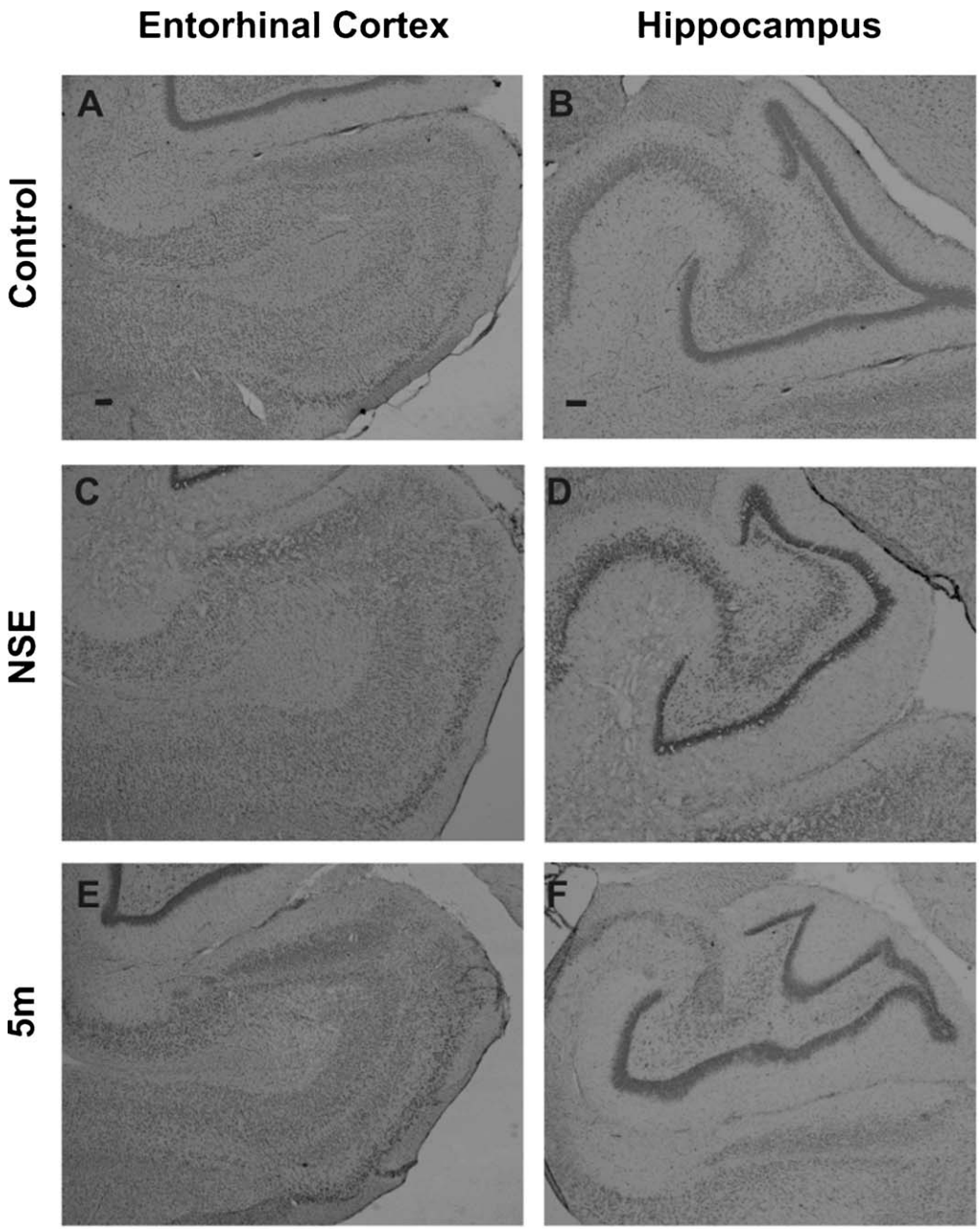

Figure 6 Malformation of DGC layer in marmosets during the chronic period after pilocarpine-induced SE. Nissl staining showing entorhinal cortex (A, C, E) and hippocampus (B, D, F) of control (A and B), NSE (C and D) and marmoset with chronic SRS (5 months after SE) (E and F). Note displacements of the DGC layer of in marmoset with SRS 5 months after pilocarpine-induced SE. There is no cell displacement or cell cluster in other hippocampal areas. Scale bars: 50 μm.

associated with intense damage in specific layers of entorhinal cortex in epileptic animals lowest dose of diazepam. Although, pilocarpine-induced SE in marmosets affected the same brain structures observed in rodents, it was less exuberant. While in rodents, 2 h of pilocarpine induced-SE produces almost complete degeneration (more than 75%) of amygdala, piriform cortex and hippocampal areas (Covolan and Mello, 2000), in marmosets the neuronal damage in these areas was less than 25%, even in some animals with prolonged SE (up to 8 h). Obviously, one might take into account that marmosets were treated with diazepam at a much earlier time point after SE onset to promote survival. By applying this strategy, the neuronal loss observed in pilocarpine induced-SE in marmosets seems to better resemble the damage found in most cases of human TLE. However, despite the overall low level of cellular degeneration in marmosets, the neuronal loss in the hilus was intense. Our data suggest that marmosets were less resistant than rodents in terms of morbidity/mortality to SE and require less severe injury to generate SRS.

The aim of the current study was not to provide an analysis of injury patterns within models but to determine (or to produce) an injury pattern that could result in SRS to create a non-human primate model of epilepsy. Thus, the

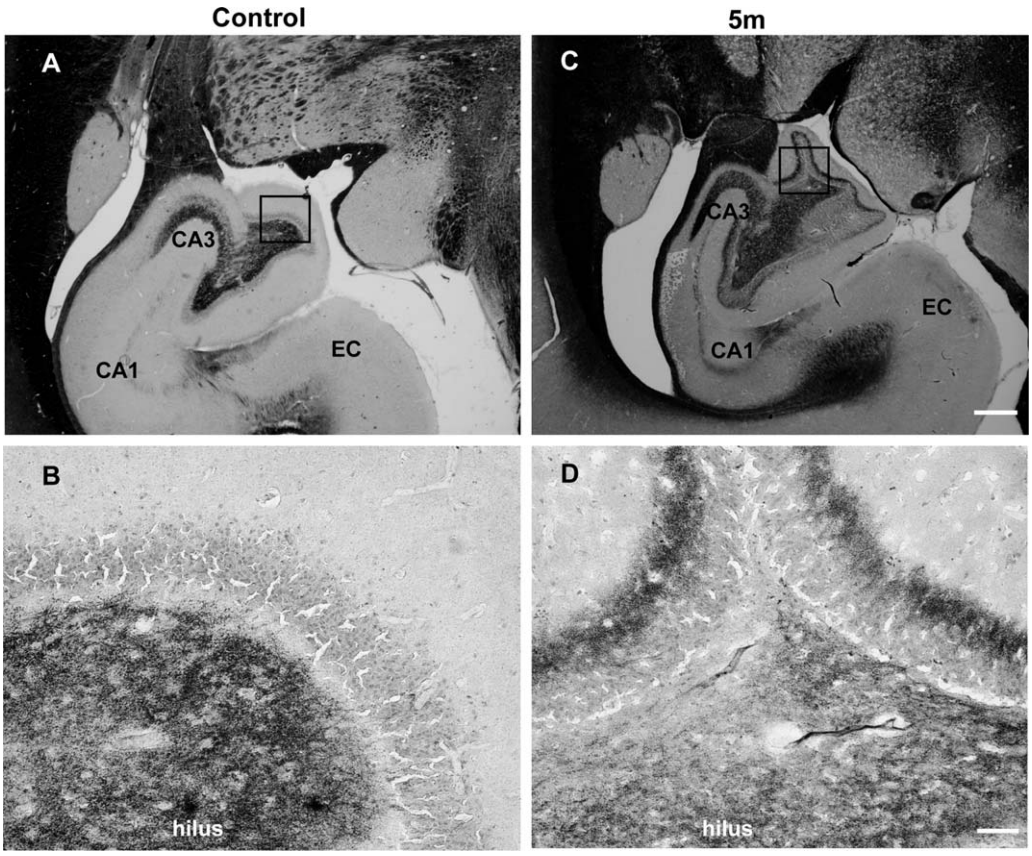

Figure 7 Mossy fiber sprouting in marmosets during the chronic period after pilocarpine-induced SE. Neo-Timm staining showing the MFS in the marmoset with chronic SRS (5 months after SE) (C and higher magnification inset with MFS in D) but not in the control (A and higher magnification inset B); scale bar: A and C: 125 μm; insets B and D: 50 μm. EC: entorhinal cortex.

determination of the injury produced by the low dose of diazepam allowed us to characterize the possible anatomical substrate (mainly in hippocampus and entorhinal cortex) underlying the generation of SRS in a non-human primate model of epilepsy.

The entorhinal cortex seems to be critically involved in TLE (Wozny et al., 2005). In patients with TLE and in several models of TLE, the entorhinal cortex shows an enhanced susceptibility to seizures (Collins et al., 1983; Spencer and Spencer, 1994). Previous studies showed that seizures cause a preferential loss of glutamatergic neurons sparing GABAergic neurons in the medial entorhinal cortex (Eid et al., 1999; Kobayashi et al., 2003). In addition selective degeneration of pyramidal neurons in regions CA1 and CA3 of the hippocampus is a common in epilepsy. Dentate granule cells and CA2 pyramidal-like neurons are relatively resistant to glutamate-induced neurodegeneration, while CA1 and CA3 pyramidal neurons were significantly more vulnerable (Mattson et al., 1989). Thus, the disrupted the feed-forward inhibition from the entorhinal cortex to a damaged hippocampal pyramidal cells facilitates the propagation of entorhinal seizures to the hippocampus, and the generation of SRS thereafter. The latency period for SRS in marmosets varied from few days to several weeks. For pilocarpine and kainate models in rodents this latent period could last a few or more days (Bumanglag and Sloviter, 2008; Leite et al., 1990; Sloviter, 2008). On the other hand, in rodent models of TLE with few hippocampal changes, such as the kindling model, SRS are either rare, taking weeks to start (Pinel, 1981). Similarly, in kindled primates, SRS developed only after several months of electrical stimulation (Wada et al., 1985; Wada and Osawa, 1976). The development of SRS and brain damage restricted mainly to the hippocampus and limbic structures are the major differences between our study and others that attempted to develop animal models of TLE using non-human primates (Gunderson et al., 1999; Soper et al., 1978; Wada and Osawa, 1976; Wada et al., 1974). The TLE model in marmosets described here reproduces the main features of TLE in humans. The use of pilocarpine in non-human primates as a model of epilepsy could provide new insights concerning the human TLE and could provide a new tool for screening of new AED. To properly evaluate the causes and consequences associated with human TLE we sought to develop a non-human primate model of temporal lobe epilepsy.

The main features of the SRS observed here resembled those of pilocarpine and kainate models of TLE in rodents and of human complex partial seizures (Leite et al., 1990; Turski et al., 1983). The brain damage seems to be restricted to the hippocampus and limbic structures during this chronic period. In human mesial TLE hippocampal atrophy on T1-weighted and mesial temporal hyper signal on T2-weighted images of MRI readily indicate the presence of hippocampal sclerosis (Cascino et al., 1991; Kuzniecky et al., 1997). Similarly, MRI performed in some marmosets with SRS showed structural changes restricted to the hippocampus, similar to the human hippocampal sclerosis.

Marmosets with SRS exhibited malformations located in the DG, characterized by invaginations and lateral displacement of the granular cell layer, mainly in the posterior plates. This alteration resembled the so called tectonic developmental malformation described previously in the hippocampus from human TLE (Sloviter et al., 2004). Different from the presumably developmental malformation found in patients with TLE with minimal hippocampal cell loss, we did not observe expansion of CA1 pyramidal cell/subicular layer that appears to compress and deform the DG adjacent to the expansion. We cannot eliminate the possibility that in humans these changes (cell dispersion of the DG and tectonic malformations) could be attributed to changes in neurodevelopment. However, our data suggest that in the adult primate, these alterations can take place after injury (SE) during adult life, even within a few months. Comparatively, while prominent in rodent SE models (Mello et al., 1992; Suzuki et al., 1995), granule cell dispersion is not as frequent in humans with TLE (Houser, 1990). Similarly, dentate neurogenesis is quite robust in rodents (Covolan et al., 2000; Parent et al., 1997) but rather discrete in adult non-human primates (Gould et al., 1999) and in humans (Eriksson et al., 1998).

MFS, another important feature in rodent models and in human TLE (Babb et al., 1991; Mello et al., 1993; Sutula et al., 1989; Tauck and Nadler, 1985), was also observed in marmosets. However, no correlation was found between MFS and seizures frequency and intensity. Whether MFS does or does not seem to be necessary for SRS development is still under debate (Longo and Mello, 1998; Pitkanen et al., 2005; Tauck and Nadler, 1985; Williams et al., 2002).

The characterization of a non-human primate model of epilepsy allows investigation of higher brain functions and subtle changes associated with epilepsy without the confounding influence of antiepileptic drugs. Finally, it may also provide a new model for antiepileptic drug screening. Altogether, our data suggest that this new model of TLE in marmosets has great resemblance to human TLE, and may provide a new tool to evaluate the causes and consequences associated with TLE.

Conflict of interest

None of the authors have any conflict of interest to disclose.

Acknowledgements

We thank Mercedes Paredes for reviewing the manuscript. Financial support Fapesp and CNPq (Brazil).

Appendix A. Supplementary data

Supplementary data associated with this article can be found, in the online version, at doi:10.1016/j.eplepsyres.2011.04.015.

References

Babb, T.L., Kupfer, W.R., Pretorius, J.K., Crandall, P.H., Levesque, M.F., 1991. Synaptic reorganization by mossy fibers in human epileptic fascia dentata. Neuroscience 42, 351—363.

Bachiega, J.C., Blanco, M.M., Perez-Mendes, P., Cinini, S.M., Covolan, L., Mello, L.E., 2008. Behavioral characterization of pentylenetetrazol-induced seizures in the marmoset. Epilepsy Behav. 13, 70—76.

Ben-Ari, Y., Tremblay, E., Ottersen, O.P., 1980. Injections of kainic acid into the amygdaloid complex of the rat: an electrographic, clinical and histological study in relation to the pathology of epilepsy. Neuroscience 5, 515—528.

Bethmann, K., Fritschy, J.M., Brandt, C., Loscher, W., 2008. Antiepileptic drug resistant rats differ from drug responsive rats in GABA A receptor subunit expression in a model of temporal lobe epilepsy. Neurobiol. Dis. 31, 169—187.

Bumanglag, A.V., Sloviter, R.S., 2008. Minimal latency to hippocampal epileptogenesis and clinical epilepsy after perforant pathway stimulation-induced status epilepticus in awake rats. J. Comp. Neurol. 510, 561—580.

Cascino, G.D., Jack Jr., C.R., Parisi, J.E., Sharbrough, F.W., Hirschorn, K.A., Meyer, F.B., Marsh, W.R., O'Brien, P.C., 1991. Magnetic resonance imaging-based volume studies in temporal lobe epilepsy: pathological correlations. Ann. Neurol. 30, 31—36.

Cavalheiro, E.A., Riche, D.A., Le Gal La Salle, G., 1982. Long-term effects of intrahippocampal kainic acid injection in rats: a method for inducing spontaneous recurrent seizures. Electroencephalogr. Clin. Neurophysiol. 53, 581—589.

Collins, R.C., Tearse, R.G., Lothman, E.W., 1983. Functional anatomy of limbic seizures: focal discharges from medial entorhinal cortex in rat. Brain Res. 280, 25—40.

Covolan, L., Mello, L.E., 2000. Temporal profile of neuronal injury following pilocarpine or kainic acid-induced status epilepticus. Epilepsy Res. 39, 133—152.

Covolan, L., Ribeiro, L.T., Longo, B.M., Mello, L.E., 2000. Cell damage and neurogenesis in the dentate granule cell layer of adult rats after pilocarpine- or kainate-induced status epilepticus. Hippocampus 10, 169—180.

Cunha, A.O., Mortari, M.R., Liberato, J.L., dos Santos, W.F., 2009. Neuroprotective effects of diazepam, carbamazepine, phenytoin and ketamine after pilocarpine-induced status epilepticus. Basic Clin. Pharmacol. Toxicol. 104, 470—477.

Dolorfo, C.L., Amaral, D.G., 1998. Entorhinal cortex of the rat: organization of intrinsic connections. J. Comp. Neurol. 398, 49—82.

Doucette, T.A., Bernard, P.B., Husum, H., Perry, M.A., Ryan, C.L., Tasker, R.A., 2004. Low doses of domoic acid during postnatal development produce permanent changes in rat behaviour and hippocampal morphology. Neurotoxicol. Res. 6, 555—563.

Eid, T., Schwarcz, R., Ottersen, O.P., 1999. Ultrastructure and immunocytochemical distribution of GABA in layer III of the rat medial entorhinal cortex following aminooxyacetic acid-induced seizures. Exp. Brain Res. 125, 463—475.

Engel, J.J., Pedley, T., 1997. What is epilepsy? In: Engel, J.J., Pedley, T. (Eds.), Epilepsy: A Comprehensive Textbook. Lippincott Williams and Wilkins, pp. 1—7.

Eriksson, P.S., Perfilieva, E., Bjork-Eriksson, T., Alborn, A.M., Nordborg, C., Peterson, D.A., Gage, F.H., 1998. Neurogenesis in the adult human hippocampus. Nat. Med. 4, 1313—1317.

Gallyas, F., Zoltay, G., Dames, W., 1992. Formation of ''dark'' (argyrophilic) neurons of various origin proceeds with a common mechanism of biophysical nature (a novel hypothesis). Acta Neuropathol. 83, 504—509.

Gao, X.G., Liu, Y., Liu, X.Z., 2007. Treatment of late lithium-pilocarpine-induced status epilepticus with diazepam. Epilepsy Res. 74, 126—130.

Goddard, G.V., 1967. Development of epileptic seizures through brain stimulation at low intensity. Nature 214, 1020—1021.

Goffin, K., Nissinen, J., Van Laere, K., Pitkanen, A., 2007. Cyclicity of spontaneous recurrent seizures in pilocarpine model of temporal lobe epilepsy in rat. Exp. Neurol. 205, 501—505.

Gould, E., Reeves, A.J., Graziano, M.S., Gross, C.G., 1999. Neurogenesis in the neocortex of adult primates. Science 286, 548—552.

Gunderson, V.M., Dubach, M., Szot, P., Born, D.E., Wenzel, H.J., Maravilla, K.R., Zierath, D.K., Robbins, C.A., Schwartzkroin, P.A., 1999. Development of a model of status epilepticus in pigtailed macaque infant monkeys. Dev. Neurosci. 21, 352—364.

Hellier, J.L., Patrylo, P.R., Buckmaster, P.S., Dudek, F.E., 1998. Recurrent spontaneous motor seizures after repeated low-dose systemic treatment with kainate: assessment of a rat model of temporal lobe epilepsy. Epilepsy Res. 31, 73—84.

Houser, C.R., 1990. Granule cell dispersion in the dentate gyrus of humans with temporal lobe epilepsy. Brain Res. 535, 195—204.

Ishida, K., Ungusparkorn, C., Hida, H., Aihara, N., Ida, K., Nishino, H., 1999. Argyrophilic dark neurons distribute with a different pattern in the brain after over hours treadmill running and swimming in the rat. Neurosci. Lett. 277, 149—152.

Kloosterman, F., Van Haeften, T., Witter, M.P., Lopes Da Silva, F.H., 2003. Electrophysiological characterization of interlaminar entorhinal connections: an essential link for re-entrance in the hippocampal-entorhinal system. Eur. J. Neurosci. 18, 3037—3052.

Kobayashi, M., Wen, X., Buckmaster, P.S., 2003. Reduced inhibition and increased output of layer II neurons in the medial entorhinal cortex in a model of temporal lobe epilepsy. J. Neurosci. 23, 8471—8479.

Kohler, C., 1986. Intrinsic connections of the retrohippocampal region in the rat brain II. The medial entorhinal area. J. Comp. Neurol. 246, 149—169.

Kuzniecky, R.I., Bilir, E., Gilliam, F., Faught, E., Palmer, C., Morawetz, R., Jackson, G., 1997. Multimodality MRI in mesial temporal sclerosis: relative sensitivity and specificity. Neurology 49, 774—778.

Leite, J.P., Bortolotto, Z.A., Cavalheiro, E.A., 1990. Spontaneous recurrent seizures in rats: an experimental model of partial epilepsy. Neurosci. Biobehav. Rev. 14, 511—517.

Lemos, T., Cavalheiro, E.A., 1996. Status epilepticus and the late development of spontaneous seizures in the pilocarpine model of epilepsy. Epilepsy. Res., 137—144 (Suppl. 2).

Longo, B.M., Mello, L.E., 1998. Supragranular mossy fiber sprouting is not necessary for spontaneous seizures in the intrahippocampal kainate model of epilepsy in the rat. Epilepsy Res. 32, 172—182.

Mattson, M.P., Guthrie, P.B., Kater, S.B., 1989. Intrinsic factors in the selective vulnerability of hippocampal pyramidal neurons. Prog. Clin. Biol. Res. 317, 333—351.

McNamara, J.O., 1986. Kindling model of epilepsy. Adv. Neurol. 44, 303—318.

Mello, L.E., Cavalheiro, E.A., Tan, A.M., Kupfer, W.R., Pretorius, J.K., Babb, T.L., Finch, D.M., 1993. Circuit mechanisms of seizures in the pilocarpine model of chronic epilepsy: cell loss and mossy fiber sprouting. Epilepsia 34, 985—995.

Mello, L.E., Cavalheiro, E.A., Tan, A.M., Pretorius, J.K., Babb, T.L., Finch, D.M., 1992. Granule cell dispersion in relation to mossy fiber sprouting, hippocampal cell loss, silent period and seizure frequency in the pilocarpine model of epilepsy. Epilepsy Res. 51—59 (Suppl. 9), 59—60 (discussion).

Parent, J.M., Yu, T.W., Leibowitz, R.T., Geschwind, D.H., Sloviter, R.S., Lowenstein, D.H., 1997. Dentate granule cell neurogenesis is increased by seizures and contributes to aberrant network reorganization in the adult rat hippocampus. J. Neurosci. 17, 3727—3738.

Perez-Mendes, P., Cinini, S.M., Medeiros, M.A., Tufik, S., Mello, L.E., 2005. Behavioral and histopathological analysis of domoic Acid administration in marmosets. Epilepsia 46 (Suppl. 5), 148—151.

Perl, T.M., Bedard, L., Kosatsky, T., Hockin, J.C., Todd, E.C., Remis, R.S., 1990. An outbreak of toxic encephalopathy caused by eating mussels contaminated with domoic acid. N. Engl. J. Med. 322, 1775—1780.

Pinel, J.P., 1981. Kindling-induced experimental epilepsy in rats: cortical stimulation. Exp. Neurol. 72, 559—569.

Pinel, J.P., Rovner, L.I., 1978. Experimental epileptogenesis: kindling-induced epilepsy in rats. Exp. Neurol. 58, 190—202.

Pitkanen, A., Kharatishvili, I., Narkilahti, S., Lukasiuk, K., Nissinen, J., 2005. Administration of diazepam during status epilepticus reduces development and severity of epilepsy in rat. Epilepsy Res. 63, 27—42.

Racine, R., Okujava, V., Chipashvili, S., 1972. Modification of seizure activity by electrical stimulation. 3. Mechanisms. Electroencephalogr. Clin. Neurophysiol. 32, 295—299.

Scallet, A.C., Binienda, Z., Caputo, F.A., Hall, S., Paule, M.G., Rountree, R.L., Schmued, L., Sobotka, T., Slikker Jr., W., 1993. Domoic acid-treated cynomolgus monkeys (*M. fascicularis*): effects of dose on hippocampal neuronal and terminal degeneration. Brain Res. 627, 307—313.

Sloviter, R.S., 2008. Hippocampal epileptogenesis in animal models of mesial temporal lobe epilepsy with hippocampal sclerosis: the importance of the ''latent period'' and other concepts. Epilepsia 49 (Suppl. 9), 85—92.

Sloviter, R.S., Kudrimoti, H.S., Laxer, K.D., Barbaro, N.M., Chan, S., Hirsch, L.J., Goodman, R.R., Pedley, T.A., 2004. ''Tectonic'' hippocampal malformations in patients with temporal lobe epilepsy. Epilepsy Res. 59, 123—153.

Soper, H.V., Strain, G.M., Babb, T.L., Lieb, J.P., Crandall, P.H., 1978. Chronic alumina temporal lobe seizures in monkeys. Exp. Neurol. 62, 99—121.

Spencer, S.S., Spencer, D.D., 1994. Entorhinal-hippocampal interactions in medial temporal lobe epilepsy. Epilepsia 35, 721—727.

Stephan, H., Baron, G., Schwerdtfeger, W.K., 1980. The Brain of the Common Marmoset (*Callithrix jacchus*): A Stereotaxic Atlas the Brain of the Common Marmoset (*Callithrix jacchus*): A Stereotaxic Atlas. Springer Verlag.

Sutula, T., Cascino, G., Cavazos, J., Parada, I., Ramirez, L., 1989. Mossy fiber synaptic reorganization in the epileptic human temporal lobe. Ann. Neurol. 26, 321—330.

Suzuki, F., Junier, M.P., Guilhem, D., Sorensen, J.C., Onteniente, B., 1995. Morphogenetic effect of kainate on adult hippocampal neurons associated with a prolonged expression of brain-derived neurotrophic factor. Neuroscience 64, 665—674.

Tasker, R.A., Strain, S.M., Drejer, J., 1996. Selective reduction in domoic acid toxicity in vivo by a novel non-N-methyl-D-aspartate receptor antagonist. Can. J. Physiol. Pharmacol. 74, 1047—1054.

Tauck, D.L., Nadler, J.V., 1985. Evidence of functional mossy fiber sprouting in hippocampal formation of kainic acid-treated rats. J. Neurosci. 5, 1016—1022.

Treiman, D.M., Meyers, P.D., Walton, N.Y., Collins, J.F., Colling, C., Rowan, A.J., Handforth, A., Faught, E., Calabrese, V.P., Uthman, B.M., Ramsay, R.E., Mamdani, M.B., 1998. A comparison of four treatments for generalized convulsive status epilepticus. Veterans Affairs Status Epilepticus Cooperative Study Group. N. Engl. J. Med. 339, 792—798.

Tryphonas, L., Iverson, F., 1990. Neuropathology of excitatory neurotoxins: the domoic acid model. Toxicol. Pathol. 18, 165—169.

Tryphonas, L., Truelove, J., Todd, E., Nera, E., Iverson, F., 1990. Experimental oral toxicity of domoic acid in cynomolgus monkeys (*Macaca fascicularis*) and rats. Preliminary investigations. Food Chem. Toxicol. 28, 707—715.

Turski, W.A., Cavalheiro, E.A., Schwarz, M., Czuczwar, S.J., Kleinrok, Z., Turski, L., 1983. Limbic seizures produced by pilocarpine in rats: behavioural, electroencephalographic and neuropathological study. Behav. Brain Res. 9, 315—335.

van Haeften, T., Baks-te-Bulte, L., Goede, P.H., Wouterlood, F.G., Witter, M.P., 2003. Morphological and numerical analysis of synaptic interactions between neurons in deep and superficial layers of the entorhinal cortex of the rat. Hippocampus 13, 943—952.

Wada, J.A., Mizoguchi, T., Komai, S., 1985. Kindling epileptogenesis in orbital and mesial frontal cortical areas of subhuman primates. Epilepsia 26, 472—479.

Wada, J.A., Osawa, T., 1976. Spontaneous recurrent seizure state induced by daily electric amygdaloid stimulation in Senegalese baboons (*Papio papio*). Neurology 26, 273—286.

Wada, J.A., Sato, M., Corcoran, M.E., 1974. Persistent seizure susceptibility and recurrent spontaneous seizures in kindled cats. Epilepsia 15, 465—478.

Walton, N.Y., Treiman, D.M., 1988. Response of status epilepticus induced by lithium and pilocarpine to treatment with diazepam. Exp. Neurol. 101, 267—275.

Williams, P.A., Wuarin, J.P., Dou, P., Ferraro, D.J., Dudek, F.E., 2002. Reassessment of the effects of cycloheximide on mossy fiber sprouting and epileptogenesis in the pilocarpine model of temporal lobe epilepsy. J. Neurophysiol. 88, 2075—2087.

Wozny, C., Gabriel, S., Jandova, K., Schulze, K., Heinemann, U., Behr, J., 2005. Entorhinal cortex entrains epileptiform activity in CA1 in pilocarpine-treated rats. Neurobiol. Dis. 19, 451—460.